National Research Network S92

Industrial Geometry

http://www.industrial-geometry.at

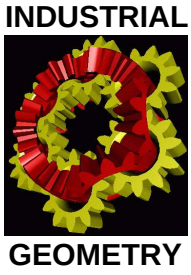

NRN Report No. 113

Shape Reconstruction with A Priori Knowledge Based on Integral Invariants

Thomas Fidler, Markus Grasmair and
Otmar Scherzer

February 2011

FWF
Der Wissenschaftsfonds.

universität wien

Shape Reconstruction with A Priori Knowledge Based on Integral Invariants

Thomas Fidler[1], Markus Grasmair[1] and Otmar Scherzer[1,2]

[1]Computational Science Center
University of Vienna
Nordbergstr. 15
1090 Vienna, Austria

[2]Radon Institute of Computational
and Applied Mathematics
Altenberger Str. 69
4040 Linz, Austria

Abstract

We investigate the applicability of integral invariants as geometrical shape descriptors in the context of ill-posed inverse problems. We propose the use of a Tikhonov functional, where the penalty term is based on the difference of integral invariants. As a case example, we consider the problem of inverting the Radon transform of an object with only limited data available. We approximate the ill-posed non-linear operator equation by a minimisation problem involving a Tikhonov functional and show existence of minimisers of the functional. Because of its non-differentiability, we derive for the numerical minimisation smooth approximations, which converge in the sense of Γ-limits.

1 Introduction

A typical task in object recognition is to segment an object in an image. In some cases, however, the image is not directly accessible, but only a transformed version of the image, e.g. its Radon transform which may occur if the object is inspected with a tomograph. Thus, the information of interest — the objects within the image — has to be reconstructed from the given data set. In mathematical terms, this task can be formulated as the inverse problem of solving an operator equation of the form

$$F[\Omega] = y,$$

where F describes the action of the tomograph on the object Ω and y denotes the available data.

The previous operator equation is a typical example of an ill-posed problem: the solution does not depend continuously on the data y. In addition, to ensure that biological harm caused by the radiation is reduced to a minimum, it might be advisable to perform the scan only for a limited number of directions. Then, it is well known from theory that the recorded data is insufficient for a unique reconstruction of the object, unless ample prior information is available. In order to stabilise the reconstruction process, the original operator equation has to be modified. A common approach is the reformulation of the operator equation

as a functional with a fit-to-data term and a regularisation term. The fit-to-data term ensures that the solution closely matches the given data, and the additionally introduced regularisation term incorporates some knowledge on the solution while at the same time enforcing well-posedness.

Typically, the a priori knowledge can be formulated as a regularity constraint on the solution. As an example, for segmenting an object in a given image, often a Tikhonov like functional is used, where the squared norm of the gradient of the boundary curve ensures the regularity of the object to be segmented. In the field of shape recovery, additionally, the a priori information may often include geometrical information about the object. Thus the regularisation term has to be constructed in such a way that the geometry of the solution is close to the geometry of the prior.

At this point, naturally, the question arises how to describe the geometry of an object in a mathematical terminology. A classical approach uses the curvature of the boundary curve of the object to define feature points, as geometrical features like protrusions, corners or inflection points can all be characterised by their curvature. All invariants, however, that are based on differentiation — thus, in particular curvature — suffer from an inherent sensitivity regarding noise. As a remedy, it has been suggested to replace differentiation by integration in such a way that the ensuing *integral invariants* still carry geometrical information about the object [4, 16, 17, 19]. These invariants have proven to be successful for object classification [16] and geometry processing [13].

This article intends to show that integral invariants can also be used for the solution of inverse problems in the context of shape recovery. To that end we propose to use a penalty term which includes the L^2-norm of the difference between the invariant of the object and the invariant of a prior. Since this penalty term is geometry based, it is expected that this procedure yields more accurate reconstructions than simpler methods based on a metric between the objects themselves, e.g. the area of the set symmetric difference or the Hausdorff distance. Indeed, the performed numerical study, which uses the Radon transform as a paradigm of an inverse problem, supports these expectations. To highlight the applicability of our method to severely ill-posed problems, we have limited the number of directions in which the Radon transform was computed to four, leading to a high number of possible solutions.

In Section 2 we briefly recall the notion of shapes and introduce the concept of integral invariants as robust geometry based shape descriptors. Section 3 is devoted to the theoretical background of inverting the Radon transform of an object. First we introduce the problem in a strict mathematical manner, which also includes a reformulation of the problem originally posed on a class of objects as a non-linear operator equation on a Hilbert space. The resulting operator being non-differentiable, we derive a smooth approximation, which is later used in the numerical implementation. In Section 4, we perform a case study using synthetic data and compare the proposed method with a Kaczmarz method using the prior as an initial guess. Both approaches turn out to be capable of reconstructing the rough shape of the object, but the Kaczmarz method introduces artificial perturbations of the object's boundary where Tikhonov regularisation with integral invariants does not.

2 Regularisation with Integral Invariants

Suppose we have an operator $F\colon X \to Y$, which maps a shape x to some given data y, i.e.,

$$F[x] = y. \tag{1}$$

We assume that the data set y is available through some measurement setup and the underlying physical principle is described by the operator F. We focus on the inverse problem of finding a suitable shape x matching the data y. The first question arising at this point is the well-posedness of the problem. The failure of well-posedness may be due to various reasons, e.g. discontinuity of the inverse operator. In this article we mainly consider one specific type of ill-posedness in the area of inverse problems: multiple solutions because of incomplete or insufficient data.

Assuming that the available data y is insufficient to solve the equation (1) uniquely, we have to regularise the original operator equation. In shape optimisation and reconstruction a common approach to stabilising the process of solving (1) is to use a prior incorporating some knowledge of the solution. The prior can be seen as a reference model that covers the essential information about the object. A typical choice is some representative of the shape, generated from a set of training data using statistical methods. In that context the possible variations of the shapes are explained in terms of statistics, e.g. using a principal component analysis where the shapes are points on a possible infinite dimensional manifold [5, 7, 21](see also [18]). In contrast, we propose to use integral invariants to explain and handle the variability of a shape. This concept has been applied successfully to segmentation with priors [17], but not yet for more general inverse and ill-posed problems.

In the following we will briefly introduce the concept of shapes and integral invariants.

2.1 Shapes

We consider a shape as a characteristic function of a given simply connected and bounded set $\Omega \subset \mathbb{R}^2$. In addition, we restrict ourselves to objects that are star-shaped with respect to the origin and therefore can be represented by a non-negative radial function.

Definition 1. Let $\gamma \in L^2(\mathbb{S}^1, \mathbb{R}_+) := \big\{\gamma \in L^2(\mathbb{S}^1, \mathbb{R}) : \gamma \geq 0\big\}$. The set

$$\Omega_\gamma := \big\{t\tau \in \mathbb{R}^2 : \tau \in \mathbb{S}^1,\ 0 \leq t \leq \gamma(\tau)\big\} \tag{2}$$

is called the *domain* generated by the non-negative radial function γ. ■

Notice that the assumption $\gamma \in L^2(\mathbb{S}^1, \mathbb{R}_+)$ is necessary (and sufficient) to guarantee that the object Ω_γ has a finite area. Indeed, a short calculation reveals that

$$\mathcal{L}^2(\Omega_\gamma) = \frac{1}{2}\int_{\mathbb{S}^1} \gamma^2(\tau)\, d\mathcal{H}^1(\tau) = \frac{1}{2}\|\gamma\|_{L^2}^2 < \infty,$$

where $\mathcal{L}^2$ and $\mathcal{H}^1$ denote the Lebesgue and the Hausdorff measure, respectively.

An intuitive definition of shapes was given by Kendall [14, p. 2]: a shape is *"what is left when the differences which can be attributed to translations, rotations, and dilatations have been quotiented out."* In contrast, by our definition

the shape changes if one applies a rigid body motion. Hence, it would be more common to use the notion of objects rather than that of shapes. But at least we have retained some invariance with respect to rotations (cf. Definition 2): a rotation of Ω_γ simply corresponds to a shift of the argument of the radial function γ.

2.2 Integral Invariants

We now briefly repeat the concept of integral invariants and introduce the circular integral invariant, which has proven to be useful in applications. A reader interested in this topic may find useful background information in the articles of Manay et al. [16] or in [3, 4].

The basic idea of integral invariants is closely related to that of differential invariants, but with an emphasis on stability with respect to noise. In contrast to differential invariants (cf. [1]), which are based on derivatives, the key to noise insensitivity of integral invariants is the replacement of differentiation by integration. Apart from that, the main features of differential invariants should be retained, e.g. a possible geometrical interpretation or invariance with respect to some group operation. In case of the curvature of the boundary curve of a sufficiently regular object — the most common representative of differential invariants — we have an obvious geometrical interpretation and also invariance with respect to rigid body motions. More precisely, invariance holds if understood in the following sense:

Definition 2. A mapping $I\colon L^2(\mathbb{S}^1,\mathbb{R}_+) \to L^1(\mathbb{S}^1,\mathbb{R}_+)$ is *invariant* with respect to the group of rotations $SO(2)$ if

$$I[\gamma](\tau) = I[\gamma \circ h](h\tau) \quad \text{for all } h \in SO(2). \tag{3}$$

■

In [19] it has been shown that the area of the intersection of an object with a ball centred at its boundary is closely related to the curvature of the boundary of the object. This provides a motivation for the following definition of the circular integral invariant first introduced by Manay et al. [16].

Definition 3. Let $R > 0$ and define $B_R(x) := \{y \in \mathbb{R}^2 : \|x - y\|_2 < R\}$. The operator $\mathcal{I}_R\colon L^2(\mathbb{S}^1,\mathbb{R}_+) \to L^1(\mathbb{S}^1,\mathbb{R}_+)$ defined by

$$\mathcal{I}_R[\gamma](\tau) := \mathcal{L}^2\Big(\Omega_\gamma \cap B_R\big(\gamma(\tau)\tau\big)\Big), \tag{4}$$

where Ω_γ denotes the domain generated by the radial function γ (see Definition 1), is called the *circular integral invariant* (cf. Figure 1). ■

Theorem 4. *The circular integral invariant of Definition 3 is continuous.*

Proof. Assume that γ_k converges to γ in $L^2(\mathbb{S}^1,\mathbb{R}_+)$. Then we obtain for almost every $\tau \in \mathbb{S}^1$ that $\gamma_k(\tau) \to \gamma(\tau)$. As a consequence, we see that for almost every $\tau \in \mathbb{S}^1$ we have that $\chi_{B_R(\gamma_k(\tau)\tau)} \to \chi_{B_R(\gamma(\tau)\tau)}$ pointwise almost everywhere. In addition, we know that $\chi_{\Omega_{\gamma_k}}$ converges pointwise almost everywhere to χ_{Ω_γ} and, consequently, for almost every $\tau \in \mathbb{S}^1$,

$$\chi_{\Omega_{\gamma_k}}\chi_{B_R(\gamma_k(\tau)\tau)} \to \chi_{\Omega_\gamma}\chi_{B_R(\gamma(\tau)\tau)} \quad \text{pointwise a.e.}$$

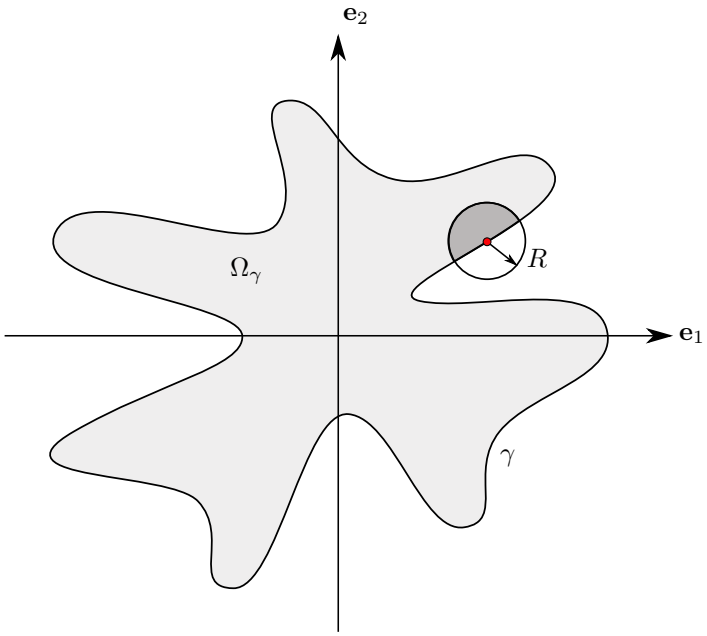

Figure 1: Visualisation of the definition of the circular integral invariant.

Applying Lebesgue's Theorem of Dominated Convergence twice, we see that

$$\int_{\mathbb{S}^1} \left|\mathcal{I}_R[\gamma](\tau) - \mathcal{I}_R[\gamma_k](\tau)\right| d\mathcal{H}^1(\tau) =$$
$$\int_{\mathbb{S}^1} \left| \int_{\mathbb{R}^2} \chi_{\Omega_\gamma \cap B_R(\gamma(\tau)\tau)}(x)\, d\mathcal{L}^2(x) - \int_{\mathbb{R}^2} \chi_{\Omega_{\gamma_k} \cap B_R(\gamma_k(\tau)\tau)}(x)\, d\mathcal{L}^2(x) \right| d\mathcal{H}^1(\tau) \to 0,$$

which concludes the proof. □

A more detailed discussion of the circular integral invariant is presented in [4]. In addition, one can find there an explicit formula in terms of the radial function (cf. [4, Lemma 4.2]). The same formula is used for the implementation of the invariant in the numerical examples below. Also, the Radon transform of a star-shaped object, the stable approximate inversion of which is considered in our case example, is rewritten in terms of the radial function. This enables us to work within the functional analytic setting of the Hilbert space $L^2(\mathbb{S}^1, \mathbb{R})$.

3 Example: Shape Reconstruction based on the Radon Transform

In this section we consider the problem of reconstructing an object from a given data set that represents the Radon transform of the object in some predefined directions. More mathematically, this task can be formulated as an inverse problem as follows: Find an object Ω such that its Radon transform $\mathbf{R}_{\sigma_i}$ for finitely many given directions σ_i, $i = 1, \ldots, n$, matches the data y_i. I.e., find a

solution of

$$\mathbf{R}_{\sigma_i}[\Omega] = y_i, \quad i = 1, \dots, n. \tag{5}$$

Since we are given only finitely many directions, the problem of solving (5) is ill-posed, and therefore we have to apply some regularisation incorporating a priori information about the geometry of the objects to be reconstructed. In the following we show how information based on integral invariants can be used in a Tikhonov like regularisation method on the set of all non-negative radial functions generating star-shaped objects. In particular, we end up with a shape optimisation problem, where the admissible shapes are restricted to those that can be represented by a non-negative radial function. Similar inverse problems for star-shaped objects have been considered by Hettlich and Rundell (cf. [9–11]) using different approaches to stabilise the inversion, among them iterative schemes and also Tikhonov regularisation. In contrast to their proposed methods including only smoothness assumptions, we explicitly incorporate additional geometric information by means of the circular integral invariant.

3.1 The Optimisation Problem

We now reformulate the geometrical definition of the standard Radon transform in terms of the generating radial function. For that purpose we introduce an operator $\mathcal{R}_{\sigma_i}$ that first maps the radial function γ to the object it generates, and afterwards applies to this object the standard Radon transform restricted to a specific direction $\sigma_i \in \mathbb{S}^1$.

Definition 5. Let $\sigma_i \in \mathbb{S}^1$ and define the operator $\mathcal{R}_{\sigma_i} \colon L^2(\mathbb{S}^1, \mathbb{R}_+) \to L^1(\mathbb{R}, \mathbb{R})$ by

$$\mathcal{R}_{\sigma_i}[\gamma](\alpha) := \int_{\mathbb{R}} \chi_{\Omega_\gamma}(\alpha\sigma_i^{\perp} + t\sigma_i)\, d\mathcal{L}^1(t). \tag{6}$$

■

Notice that the geometrical interpretation of $\mathcal{R}_{\sigma_i}[\gamma]$ and the standard Radon transform of Ω_γ coincide. The major difference is the non-linearity of $\mathcal{R}_{\sigma_i}$ with respect to the radial function γ.

Lemma 6. *The operator $\mathcal{R}_{\sigma_i}$ of Definition 5 is continuous.*

We now define the Tikhonov regularisation of (5) in a precise mathematical manner.

Definition 7. Let $\beta, \mu > 0$ and $\gamma_{\text{ref}} \in L^2(\mathbb{S}^1, \mathbb{R}_+)$. In addition, denote by $\mathcal{I} \colon L^2(\mathbb{S}^1, \mathbb{R}_+) \to L^1(\mathbb{S}^1, \mathbb{R}_+)$ the circular integral invariant defined by (4). For $\sigma_i \in \mathbb{S}^1$ and $f_i \in L^2(\mathbb{R}, \mathbb{R})$, $i = 1, \dots, n$, define

$$\mathcal{D}_{\sigma_i}[\gamma] := \frac{1}{2}\|\mathcal{R}_{\sigma_i}[\gamma] - f_i\|_{L^2}^2 \quad \text{and} \quad \mathcal{P}[\gamma] := \frac{1}{2}\big(\|\mathcal{I}[\gamma] - \mathcal{I}[\gamma_{\text{ref}}]\|_{L^2}^2 + \mu\|\gamma'\|_{L^2}^2\big),$$

and the functional $\mathcal{F} \colon L^2(\mathbb{S}^1, \mathbb{R}) \to \mathbb{R} \cup \{+\infty\}$ by

$$\mathcal{F}[\gamma] := \begin{cases} \displaystyle\sum_{i=1}^{n} \mathcal{D}_{\sigma_i}[\gamma] + \beta\mathcal{P}[\gamma] & \text{if } \gamma \in H^1(\mathbb{S}^1, \mathbb{R}_+), \\ +\infty & \text{else.} \end{cases} \tag{7}$$

■

The operator $\mathcal{R}_{\sigma_i}$ is defined for a function depending on values on $\mathbb{S}^1$. Therefore, its evaluation at a specific point α should be written as an integral over a subset of $\mathbb{S}^1$ as well. A simple parameter transform yields the following reformulation of the operator.

Lemma 8. *Let $\sigma_i \in \mathbb{S}^1$. Denote by $H_1(x)$ the Heaviside function defined by $H_1(x) = 0$ for $x < 1$ and $H_1(x) = 1$ for $x \geq 1$, and define the half-sphere*

$$\mathbb{S}^1_{\sigma_i,\alpha} := \big\{\tau \in \mathbb{S}^1 : \operatorname{sign}(\langle \tau, \sigma_i^\perp \rangle) = \operatorname{sign}(\alpha)\big\}.$$

The operator $\mathcal{R}_{\sigma_i}$ of Definition 5 can be written as

$$\mathcal{R}_{\sigma_i}[\gamma](\alpha) = \begin{cases} \displaystyle\int_{\mathbb{S}^1_{\sigma_i,\alpha}} H_1\Big(\frac{\gamma(\tau)\langle \tau, \sigma_i^\perp\rangle}{\alpha}\Big) \frac{|\alpha|}{\langle \tau, \sigma_i^\perp\rangle^2}\, d\mathcal{H}^1(\tau), & \alpha \neq 0, \\ \gamma(\sigma_i) + \gamma(-\sigma_i), & \alpha = 0. \end{cases} \tag{8}$$

Proof. Let $\alpha \in \mathbb{R} \setminus \{0\}$ and $\sigma_i \in \mathbb{S}^1$ fixed. Define $f_{\sigma_i,\alpha} \colon \mathbb{S}^1_{\sigma_i,\alpha} \to \mathbb{R}$ by

$$f_{\sigma_i,\alpha}(\tau) := \frac{\langle \tau, \sigma_i\rangle}{\langle \tau, \sigma_i^\perp\rangle}\alpha.$$

That is, $f_{\sigma_i,\alpha}$ maps a direction $\tau \in \mathbb{S}^1_{\sigma_i,\alpha}$ to the line parallel to σ_i with offset α (see Figure 2). A short calculation shows that $\|Df_{\sigma_i,\alpha}(\tau)\| = |\alpha|/\langle \tau, \sigma_i^\perp\rangle^2$ and, as a consequence, we obtain

$$\begin{aligned} &\int_{\mathbb{S}^1_{\sigma_i,\alpha}} H_1\Big(\frac{\gamma(\tau)\langle \tau, \sigma_i^\perp\rangle}{\alpha}\Big) \frac{|\alpha|}{\langle \tau, \sigma_i^\perp\rangle^2}\, d\mathcal{H}^1(\tau) \\ &\qquad = \int_{\mathbb{R}} \left(\int_{f^{-1}_{\sigma_i,\alpha}(t) \cap \mathbb{S}^1_{\sigma_i,\alpha}} H_1\Big(\frac{\gamma(\tau)\langle \tau, \sigma_i^\perp\rangle}{\alpha}\Big)\, d\mathcal{H}^0(\tau) \right) d\mathcal{H}^1(t) \\ &\qquad = \int_{\mathbb{R}} H_1\Big(\frac{\gamma\big(f^{-1}_{\sigma_i,\alpha}(t)\big)\langle f^{-1}_{\sigma_i,\alpha}(t), \sigma_i^\perp\rangle}{\alpha}\Big)\, d\mathcal{L}^1(t). \end{aligned}$$

Thus, the assertion follows from the fact that (see Figure 2)

$$\big\{t \in \mathbb{R} : \gamma\big(f^{-1}_{\sigma_i,\alpha}(t)\big)\langle f^{-1}_{\sigma_i,\alpha}(t), \sigma_i^\perp\rangle/\alpha \geq 1\big\} = \big\{t \in \mathbb{R} : \alpha\sigma_i^\perp + t\sigma_i \in \Omega_\gamma\big\}. \quad \square$$

The optimality condition for (7) involves the derivative of the functional $\mathcal{R}_{\sigma_i}$, which, however, is not differentiable, because the integrand is the shifted Heaviside function H_1. For the numerical implementation of the minimizing procedure we replace the original functional $\mathcal{F}$ by a differentiable version $\mathcal{F}_\varepsilon$ based on a smoothed approximation of $\mathcal{R}_{\sigma_i}$.

Definition 9. Let $0 < \varepsilon < 1$ and $\sigma_i \in \mathbb{S}^1$ be fixed. Define the operator $\mathcal{R}_{\sigma_i,\varepsilon} \colon L^2(\mathbb{S}^1, \mathbb{R}_+) \to L^1(\mathbb{R}, \mathbb{R}_+)$ by

$$\mathcal{R}_{\sigma_i,\varepsilon}[\gamma](\alpha) := \begin{cases} \displaystyle\int_{\mathbb{S}^1_{\sigma_i,\alpha}} H_{1,\varepsilon}\Big(\frac{\gamma(\tau)\langle \tau, \sigma_i^\perp\rangle}{\alpha}\Big) \frac{|\alpha|}{\langle \tau, \sigma_i^\perp\rangle^2}\, d\mathcal{H}^1(\tau), & \alpha \neq 0, \\ \gamma(\sigma_i) + \gamma(-\sigma_i), & \alpha = 0. \end{cases} \tag{9}$$

Here, $H_{1,\varepsilon}$ denotes the mollification of the shifted Heaviside function. ∎

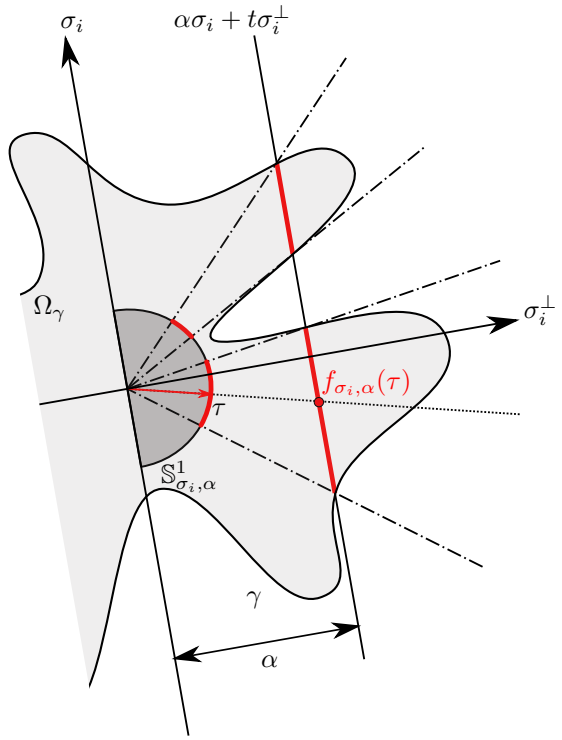

Figure 2: Sketch of the parameter transform $f_{\sigma_i,\alpha}$.

Definition 10. Let $\beta, \mu > 0$ and $\gamma_{\text{ref}} \in L^2(\mathbb{S}^1, \mathbb{R}_+)$. In addition, denote by $\mathcal{I}\colon L^2(\mathbb{S}^1, \mathbb{R}_+) \to L^2(\mathbb{S}^1, \mathbb{R}_+)$ the circular integral invariant defined by (4). For $\sigma_i \in \mathbb{S}^1$, $f_i \in L^2(\mathbb{R}, \mathbb{R})$, $i = 1, \dots, n$, and $0 < \varepsilon < 1$ define

$$\mathcal{D}_{\sigma_i,\varepsilon}[\gamma] := \frac{1}{2}\|\mathcal{R}_{\sigma_i,\varepsilon}[\gamma] - f_i\|_{L^2}^2 \quad \text{and} \quad \mathcal{P}[\gamma] := \frac{1}{2}\big(\|\mathcal{I}[\gamma] - \mathcal{I}[\gamma_{\text{ref}}]\|_{L^2}^2 + \mu\|\gamma'\|_{L^2}^2\big),$$

and the functional $\mathcal{F}_\varepsilon\colon L^2(\mathbb{S}, \mathbb{R}) \to \mathbb{R} \cup \{+\infty\}$ by

$$\mathcal{F}_\varepsilon[\gamma] := \begin{cases} \displaystyle\sum_{i=1}^n \mathcal{D}_{\sigma_i,\varepsilon}[\gamma] + \beta\mathcal{P}[\gamma] & \text{if } \gamma \in H^1(\mathbb{S}^1, \mathbb{R}_+), \\ +\infty & \text{else.} \end{cases} \tag{10}$$

■

The existence of minimisers of the functional $\mathcal{F}$ and its approximation $\mathcal{F}_\varepsilon$ is guaranteed by the following theorem.

Theorem 11. *The functionals $\mathcal{F}$ and $\mathcal{F}_\varepsilon$ of Definitions 7 and 10 are lower semi-continuous and coercive.*

Proof. We only show the lower semi-continuity and the coercivity of $\mathcal{F}_\varepsilon$, the proof for $\mathcal{F}$ being analogous.

Theorem 6.49 in [6] implies continuity of the mapping $\gamma \mapsto \mathcal{R}_{\sigma_i,\varepsilon}[\gamma](\alpha)$ for every $\alpha \in \mathbb{R}$. As a consequence, applying Fatou's Lemma, we obtain lower semi-continuity of $\mathcal{R}_{\sigma_i,\varepsilon}$. Proposition 10.7 in [20] shows lower semi-continuity of the smoothing term, and continuity of the integral invariant (see Theorem 4) in particular implies lower semi-continuity.

It remains to show that the functional $\mathcal{F}_\varepsilon$ is coercive. In the following we show that every level set of $\mathcal{F}_\varepsilon$ is bounded in $H^1(\mathbb{S}^1,\mathbb{R})$, and therefore, by the Rellich–Kondrašov Theorem (see [20, p. 258]), pre-compact in $L^2(\mathbb{S}^1,\mathbb{R})$. Let therefore $t>1$ and $\gamma\in L^2(\mathbb{S}^1,\mathbb{R})$ such that $\mathcal{F}_\varepsilon[\gamma]\le t$. Then in particular we know that $\gamma\in H^1(\mathbb{S}^1,\mathbb{R})\subset W^{1,1}(\mathbb{S}^1,\mathbb{R})$. By Theorem 18.17 in [12] we obtain for $\varphi_1,\varphi_2\in[0,2\pi[$

$$|\gamma(\varphi_1)-\gamma(\varphi_2)|\le\left|\int_{\varphi_1}^{\varphi_2}\gamma'(\varphi)\,d\mathcal{L}^1(\varphi)\right|\le\int_{\mathbb{S}^1}|\gamma'(\tau)|\,d\mathcal{H}^1(\tau)=\|\gamma'\|_{L^1(\mathbb{S}^1,\mathbb{R})}$$

and, in particular,

$$|\max_{\tau\in\mathbb{S}^1}\gamma(\tau)-\min_{\tau\in\mathbb{S}^1}\gamma(\tau)|\le\|\gamma'\|_{L^1(\mathbb{S}^1,\mathbb{R})}\le\sqrt{2\pi}\,\|\gamma'\|_{L^2(\mathbb{S}^1,\mathbb{R})}\le 2\sqrt{\frac{\pi t}{\beta\mu}}. \tag{11}$$

Let now $1\le i\le n$ be fixed. Because $f_i\in L^2(\mathbb{R},\mathbb{R})$, there exists some $\tilde r>0$ such that

$$\left(\int_{|x|>\tilde r}f_i^2(x)\,d\mathcal{L}^1(x)\right)^{1/2}<\sqrt{2}-1. \tag{12}$$

Let $r:=\max\{\tilde r,\sqrt{t}\}$. Now we show that

$$\min_{\tau\in\mathbb{S}^1}\gamma(\tau)\le(2r+1)(1+\varepsilon)\quad\text{and}\quad\max_{\tau\in\mathbb{S}^1}\gamma(\tau)\le(2r+1)(1+\varepsilon)+2\sqrt{\frac{\pi t}{\beta\mu}}. \tag{13}$$

Assume to the contrary that

$$\min\{\gamma(\tau):\tau\in\mathbb{S}^1\}>(2r+1)(1+\varepsilon). \tag{14}$$

Observe that for $0<\varepsilon<1$ we have

$$H_1\Big(\frac{t}{1+\varepsilon}\Big)\le H_{1,\varepsilon}(t)\quad\text{and thus}\quad|\mathcal{R}_{\sigma_i,\varepsilon}[\gamma](\alpha)|\ge\Big|\mathcal{R}_{\sigma_i}\Big[\frac{\gamma}{1+\varepsilon}\Big](\alpha)\Big|.$$

A simple geometrical argument (see Figure 3) shows

$$\Big|\mathcal{R}_{\sigma_i}\Big[\frac{\gamma}{1+\varepsilon}\Big](\alpha)\Big|\ge 2r\quad\text{for}\quad r<\alpha<r+1. \tag{15}$$

Define $A:=(r,r+1)$. Because $t>1$, and by (12) and (15), it follows that

$$\begin{aligned}\sqrt{t}&\ge\|\mathcal{R}_{\sigma_i,\varepsilon}[\gamma]-f_i\|_{L^2(\mathbb{R})}\ge\|\mathcal{R}_{\sigma_i,\varepsilon}[\gamma]-f_i\|_{L^2(A)}\ge\|\mathcal{R}_{\sigma_i,\varepsilon}[\gamma]\|_{L^2(A)}-\|f_i\|_{L^2(A)}\\&=\left(\int_A|\mathcal{R}_{\sigma_i,\varepsilon}[\gamma](\alpha)|^2\,d\mathcal{L}^1(\alpha)\right)^{1/2}-\|f_i\|_{L^2(A)}>2r-(\sqrt{2}-1)\\&>2\sqrt{t}-(\sqrt{2}-1)\sqrt{t}>\sqrt{t},\end{aligned}$$

which yields a contradiction to (14). Thus the first inequality in (13) holds. The second inequality is now a consequence of (11). Therefore, we can bound the L^2 norm of γ by

$$\|\gamma\|^2_{L^2(\mathbb{S}^1,\mathbb{R})}\le 2\pi\big(\max_{\tau\in\mathbb{S}^1}\gamma(\tau)\big)^2\le 2\pi\left(\big(2\max\{\tilde r,\sqrt{t}\}+1\big)(1+\varepsilon)+2\sqrt{\frac{\pi t}{\beta\mu}}\right)^2. \tag{16}$$

Together with (11), this shows that the level set of $\mathcal{F}_\varepsilon$ to the level t is bounded in $H^1(\mathbb{S}^1,\mathbb{R})$. Application of the Rellich–Kondrašov Theorem concludes the proof. □

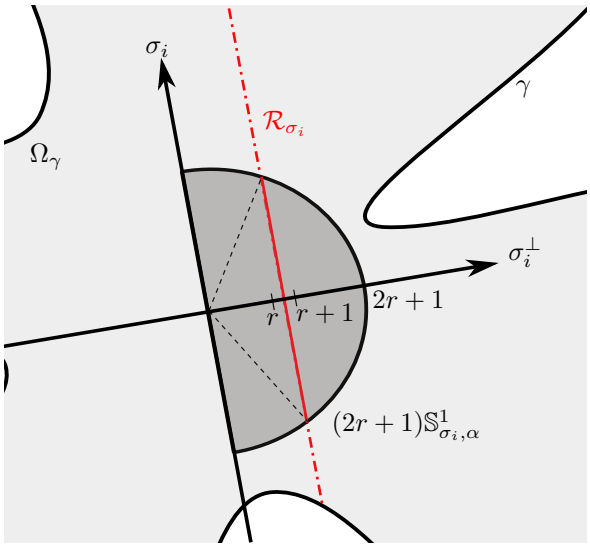

Figure 3: Sketch of estimation of $\mathcal{R}_{\sigma_i}\left[\frac{\gamma}{1+\varepsilon}\right]$ in (15).

3.2 Γ-Convergence

In this section we show that the functional $\mathcal{F}_\varepsilon$ is indeed an approximation of the original functional $\mathcal{F}$.

Lemma 12. *Let $(\varepsilon_k) \to 0$ and denote by (γ_{ε_k}) a minimising sequence of the functionals $\mathcal{F}_{\varepsilon_k}$. Then (γ_{ε_k}) has a convergent subsequence in $L^2(\mathbb{S}^1, \mathbb{R})$ and the limit of every convergent subsequence is a minimiser of $\mathcal{F}$.*

Proof. The basic idea is to prove Γ-convergence and equi-coercivity of the approximating functionals $\mathcal{F}_{\varepsilon_k}$. First notice that equi-coercivity is a direct consequence of (11) and (16) in the proof of Theorem 11.

In order to show Γ-convergence we have to verify the following two conditions (see [2, Chpt. 8]):

1. For every $\eta \in H^1(\mathbb{S}^1, \mathbb{R})$ and every sequence (η_k) in $H^1(\mathbb{S}^1, \mathbb{R})$ converging to η with respect to the L^2-norm we have
$$\mathcal{F}[\eta] \leq \liminf_{k\to\infty} \mathcal{F}_{\varepsilon_k}[\eta_k]. \tag{17}$$

2. For every $\eta \in H^1(\mathbb{S}^1, \mathbb{R})$ there exists a sequence (η_k) in $H^1(\mathbb{S}^1, \mathbb{R})$ converging to η with respect to the L^2-norm such that
$$\mathcal{F}[\eta] = \lim_{k\to\infty} \mathcal{F}_{\varepsilon_k}[\eta_k].$$

The latter condition follows immediately from the fact that $\mathcal{F}_{\varepsilon_k}[\eta]$ converges to $\mathcal{F}[\eta]$ as $k \to \infty$ for every $\eta \in L^2(\mathbb{S}^1, \mathbb{R})$.

Let $\eta \in H^1(\mathbb{S}^1, \mathbb{R})$ and let (η_k) be any sequence in $H^1(\mathbb{S}^1, \mathbb{R})$ converging to η with respect to the L^2-norm. We have to verify (17). Since the regularisation term does not depend on ε_k, this is equivalent to showing that

$\mathcal{D}_{\sigma_i}[\eta] \leq \liminf_{k\to\infty} \mathcal{D}_{\sigma_i,\varepsilon_k}[\eta_k]$ for each direction $\sigma_i \in \mathbb{S}^1$. The continuity of $\mathcal{R}_{\sigma_i}$ implies that, after possible passing to an appropriate subsequence, $\mathcal{R}_k^{\pm}(\alpha) := \mathcal{R}_{\sigma_i}[\eta_k/(1 \pm \varepsilon_k)](\alpha) \to \mathcal{R}_{\sigma_i}[\eta](\alpha)$ pointwise almost everywhere. As a consequence, applying Fatou's Lemma we obtain

$$\begin{aligned}
\liminf_{k\to\infty} \mathcal{D}_{\sigma_i,\varepsilon_k}[\eta_k] &= \liminf_{k\to\infty} \int_{\mathbb{R}} |\mathcal{R}_{\sigma_i,\varepsilon_k}[\eta_k](\alpha) - f(\alpha)|^2 \, d\mathcal{L}^1(\alpha) \\
&\geq \int_{\mathbb{R}} \liminf_{k\to\infty} |\mathcal{R}_{\sigma_i,\varepsilon_k}[\eta_k](\alpha) - f(\alpha)|^2 \, d\mathcal{L}^1(\alpha) \\
&\geq \int_{\mathbb{R}} \liminf_{k\to\infty} \Big(\min\big\{ |(\mathcal{R}_k^+ - f)(\alpha)|, |(\mathcal{R}_k^- - f)(\alpha)| \big\}^2 \Big) \, d\mathcal{L}^1(\alpha) \\
&\quad - \int_{\mathbb{R}} \limsup_{k\to\infty} \Big(|(\mathcal{R}_k^+ - \mathcal{R}_k^-)(\alpha)|^2 \Big) \, d\mathcal{L}^1(\alpha) \\
&= \int_{\mathbb{R}} |\mathcal{R}_{\sigma_i}[\eta](\alpha) - f(\alpha)|^2 \, d\mathcal{L}^1(\alpha) \\
&= \mathcal{D}_{\sigma_i}[\eta],
\end{aligned}$$

which proves the assertion. □

4 Numerical Results

The actual optimisation was performed with a gradient descent approach, which involves the derivative of the functional to minimise. Therefore we have based the numerical implementation on the smooth approximation functional $\mathcal{F}_\varepsilon$. The Γ-convergence of this functional to the original functional $\mathcal{F}$, shown in the previous section, implies that for a sufficiently small value of the smoothing parameter ε we obtain a solution that is close to an actual minimiser of $\mathcal{F}$. We have used a finite element approach with piecewise linear basis functions for the discretisation of the regularisation functional. All the integrations were realised by the trapezoidal rule. The iteration was stopped as soon as the maximal absolute value of the gradient of $\mathcal{F}_\varepsilon$ was below some reasonable threshold.

For comparison, we have also implemented a Kaczmarz method for the solution of (5), using the prior as the starting value, i.e.,

$$\begin{aligned}
\gamma_0 &= \gamma_{\text{ref}}, \\
\gamma_{k+1} &= \gamma_k + \lambda (D\mathcal{R}_{\sigma_{k \bmod n},\varepsilon})^\star (\mathcal{R}_{\sigma_{k \bmod n},\varepsilon}[\gamma_k] - f_{k \bmod n}),
\end{aligned}$$

where n denotes the number of directions in which the Radon transform is given. In addition, we have added a smoothing term in each iteration step to avoid spurious oscillations in the result. Also, with this regularisation the two methods are better comparable. The regularised iteration then reads as

$$\gamma_{k+1} = \gamma_k + \lambda \Big[(D\mathcal{R}_{\sigma_{k \bmod n},\varepsilon})^\star (\mathcal{R}_{\sigma_{k \bmod n},\varepsilon}[\gamma_k] - f_{k \bmod n}) - \mu \gamma_k'' \Big]. \tag{18}$$

Notice that for the following numerical examples the constant μ was chosen much smaller than 1. Moreover, we have used the same constant μ for the regularisation method given in Definition 10.

In all the numerical examples we have tried to reconstruct an object from its Radon transform given only in four directions. This data would allow a unique

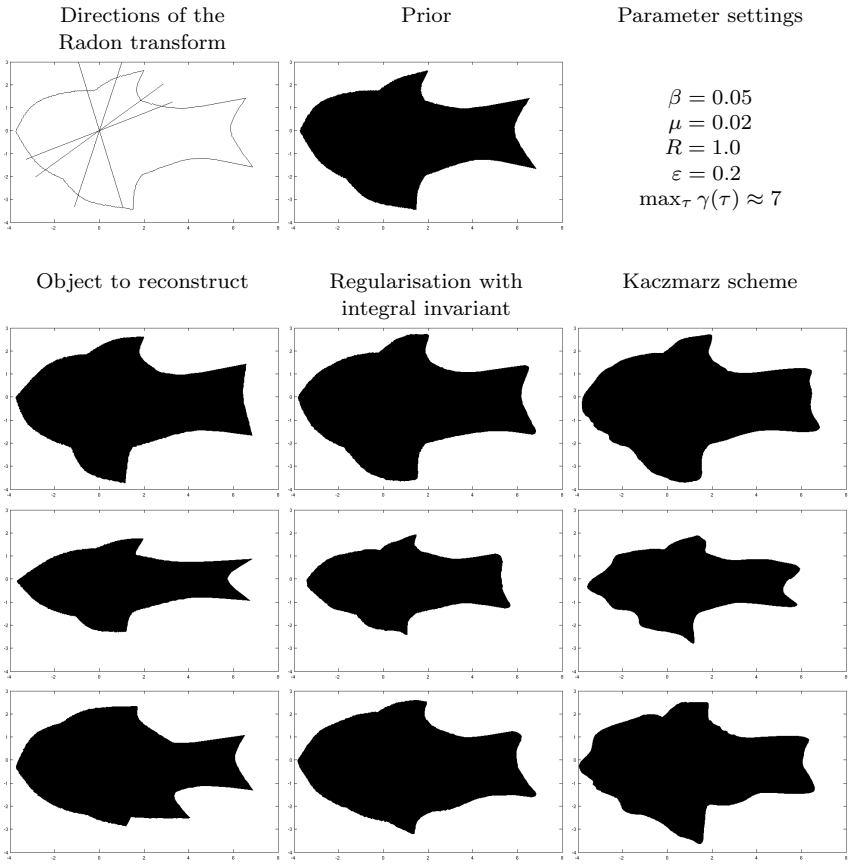

Figure 4: Reconstruction with fixed reference object (prior) shown in the first row. First column: object to reconstruct. Second column: reconstruction based on regularisation with the circular integral invariant. Third column: reconstruction based on the Kaczmarz scheme.

reconstruction if we restricted the search for solutions to the set of convex objects [8, Corollary 1.2.12]. In case of a star-shaped body, however, the same data is insufficient for a successful reconstruction [8, Theorem 2.3.4] and, consequently, the problem is ill-posed. To amplify the effect of ill-posedness we have chosen the four directions in such a way that significant parts of the object are only badly resolved (cf. Figures 4 and 5, upper left, where $\sigma_i \in \{21.6°, 36°, 72°, 108°\}$). For the numerical experiments we fixed the reference object (see Figures 4 and 5, first row) and used visually similar objects to compute artificial data sets for $\mathcal{R}_{\sigma_i,\varepsilon}$ for $i = 1, \ldots, 4$ and $\varepsilon < 1$. The results of the reconstruction with Tikhonov regularisation using the integral invariant in the prior term are depicted in Figures 4 and 5, middle column; the results of the reconstruction with the Kaczmarz scheme (18) in Figures 4 and 5, right column. In both figures the left column shows the object the data is computed from, which at the same time is the object to be reconstructed.

As can be seen from the figures, the Kaczmarz scheme produces artefacts in regions where the features of the object are badly resolved by the Radon

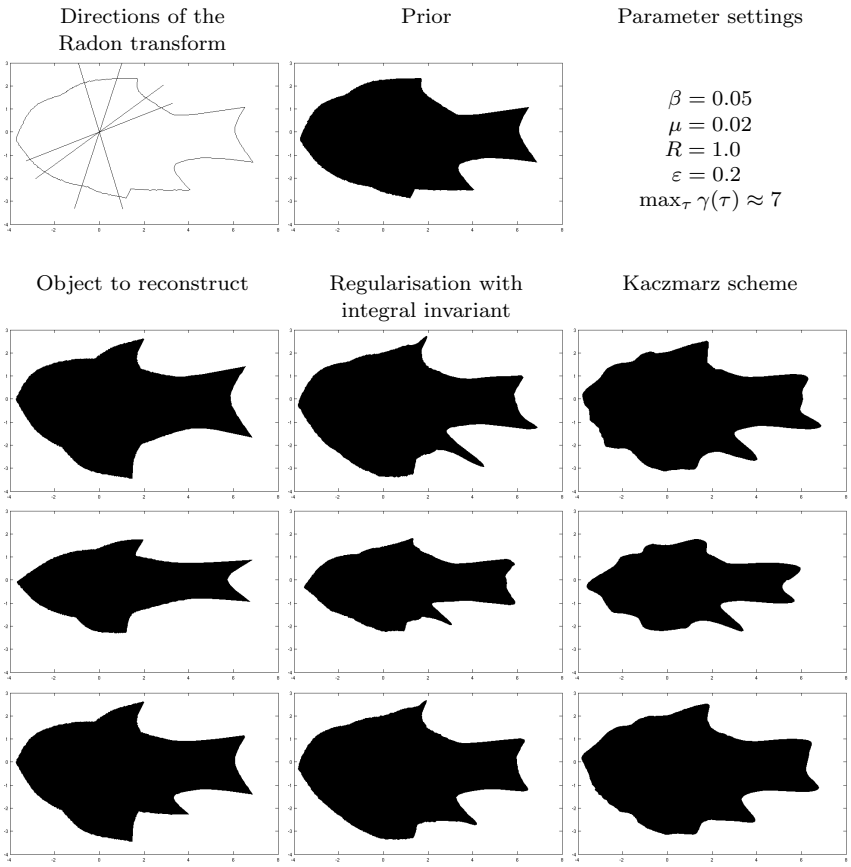

Figure 5: Reconstruction with fixed reference object (prior) shown in the first row. First column: object to reconstruct. Second column: reconstruction based on regularisation with the circular integral invariant. Third column: reconstruction based on the Kaczmarz scheme.

transform. This is quite natural, as in (18) only the data is used and the prior knowledge on the geometry of the object is solely incorporated as initial value of the iteration. In contrast, because in the badly resolved regions of the object the integral invariant of the prior covers the geometry, our method is capable to handle this lack of information and produces reconstructions that are visually more appealing. These differences can be seen best in Figure 4, last two rows: Compare in particular the shape of the fish head. Admittedly, artefacts are also present in our results, but they are limited to parts of the object where the prior information contradicts the object we want to reconstruct. Thus, the artefacts are rather due to wrong a priori knowledge than to a failure of the method. This effect occurs for instance in the first two reconstructions in Figure 5, especially at the second lower fin, which is present in the prior, but missing in the objects of interest. Thus, both, the regularisation method and the Kaczmarz scheme, try to reconstruct a feature that does not exist. Again, we want to emphasize that our method does not introduce additional artefacts in parts where the prior information is consistent with the true solution, whereas the Kaczmarz scheme does. In addition, the numerical results indicate that our method is well capable of handling scaled objects (see Figure 4, middle row), which is a consequence of the fact that the integral invariant mainly reflects curvature information of the prior [19].

5 Conclusion

In this article we have introduced a Tikhonov like regularisation functional for the reconstruction of star-shaped objects, which is based on the difference of integral invariants. As a case example, we have considered the problem of reconstructing an object from its Radon transform given only for a finite number of directions. We have derived the necessary theoretical background to show existence of minimisers of the Tikhonov functional and introduced a smooth approximation used for numerical computations. The presented numerical results indicate that the approach based on integral invariants is suitable for the reconstruction of objects in case of insufficient data. In particular, the comparison with a standard approach has shown that our method creates significantly less artefacts.

Acknowledgement

This work has been supported by the Austrian Science Fund (FWF) within the national research networks *Industrial Geometry*, project S9203-N12, and *Photoacoustic Imaging in Biology and Medicine*, project S10505-N20.

References

[1] E. Calabi, P. J. Olver, C. Shakiban, A. Tannenbaum, and S. Haker. Differential and numerically invariant signature curves applied to object recognition. *Int. J. Comput. Vision*, 26:107–135, 1998.

[2] G. Dal Maso. *An Introduction to* Γ*-Convergence*, volume 8 of *Progress in Nonlinear Differential Equations and their Applications*. Birkhäuser, 1993.

[3] T. Fidler, M. Grasmair, H. Pottmann, and O. Scherzer. Inverse problems of integral invariants and shape signatures. Reports of FSP S092 - "Industrial Geometry" 40, University of Innsbruck, Austria, 2007.

[4] T. Fidler, M. Grasmair, and O. Scherzer. Identifiability and reconstruction of shapes from integral invariants. *Inverse Probl. Imaging*, 2(3):341–354, 2008.

[5] P. T. Fletcher, C. Lu, S. M. Pizer, and S. Joshi. Principal geodesic analysis for the study of nonlinear statistics of shape. *IEEE Trans. Med. Imag.*, 23(8):995–1005, 2004.

[6] I. Fonseca and G. Leoni. *Modern methods in the calculus of variations:* L^p *spaces*. Springer Monographs in Mathematics. Springer, New York, 2007.

[7] M. Fuchs and O. Scherzer. Regularized reconstruction of shapes with statistical a priori knowledge. *Int. J. Comput. Vision*, 79(2):119–135, 2008.

[8] R. J. Gardner. *Geometric tomography*, volume 58 of *Encyclopedia of Mathematics and its Applications*. Cambridge University Press, Cambridge, second edition, 2006.

[9] F. Hettlich and W. Rundell. Iterative methods for the reconstruction of an inverse potential problem. *Inverse Probl.*, 12(3):251–266, 1996.

[10] F. Hettlich and W. Rundell. The determination of a discontinuity in a conductivity from a single boundary measurement. *Inverse Probl.*, 14:67–82, 1998.

[11] F. Hettlich and W. Rundell. Identification of a discontinuous source in the heat equation. *Inverse Probl.*, 17(5):1465–1482, 2001.

[12] E. Hewitt and K. Stromberg. *Real and Abstract Analysis*. Springer Verlag, New York, 1965.

[13] Q.-X. Huang, S. Flöry, N. Gelfand, M. Hofer, and H. Pottmann. Reassembling fractured objects by geometric matching. In *ACM SIGGRAPH 2006 Papers*, SIGGRAPH '06, pages 569–578, New York, NY, USA, 2006. ACM.

[14] D. G. Kendall. Shape manifolds, procrustean metrics and complex projective spaces. *Bull. Lond. Math. Soc.*, 16:81–121, 1984.

[15] H. Krim and A. J. Yezzi, Jr. *Statistics and Analysis of Shapes*. Birkhäuser, Boston, 2006.

[16] S. Manay, D. Cremers, B.-W. Hong, A. J. Yezzi, Jr., and S. Soatto. Integral invariants and shape matching. In *[15]*, pages 137–166, 2006.

[17] S. Manay, D. Cremers, A. J. Yezzi, Jr., and S. Soatto. One-shot integral invariant shape priors for variational segmentation. In Anand Rangarajan, Baba Vemuri, and Alan Yuille, editors, *Energy Minimization Methods in Computer Vision and Pattern Recognition*, volume 3757 of *Lecture Notes in Computer Science*, pages 414–426. Springer Berlin / Heidelberg, 2005.

[18] P. W. Michor and D. Mumford. Riemannian geometries on spaces of plane curves. *J. Eur. Math. Soc. (JEMS)*, 8:1–48, 2006.

[19] H. Pottmann, J. Wallner, Q.-X. Huang, and Y.-L. Yang. Integral invariants for robust geometry processing. *Comput. Aided Geom. Design*, 26(1):37–60, 2009.

[20] O. Scherzer, M. Grasmair, H. Grossauer, M. Haltmeier, and F. Lenzen. *Variational methods in imaging*, volume 167 of *Applied Mathematical Sciences*. Springer, New York, 2009.

[21] P. Yushkevich, P. T. Fletcher, S. Joshi, A. Thall, and S. M. Pizer. Continuous medial representations for geometric object modeling in 2D and 3D. *Image Vision Comput.*, 21(1):17 – 27, 2003.